

Study of the Process $e^+e^- \rightarrow \eta\gamma$ in c.m. Energy Range 600-1380 MeV at CMD-2

R.R. Akhmetshin*, E.V. Anashkin*, V.M. Aulchenko*[†],
 V.Sh. Banzarov*, A. Baratt[‡], L.M. Barkov*[†], S.E. Baru*[†],
 N.S. Bashtovoy*, A.E. Bondar*[†], D.V. Bondarev*, A.V. Bragin*,
 D.V. Chernyak*, S.I. Eidelman*[†], G.V. Fedotovitch*[†],
 N.I. Gabyshev*, A.A. Grebeniuk*, D.N. Grigoriev*, V.W. Hughes[§],
 F.V. Ignatov*[†], S.V. Karpov*, V.F. Kazanin*, B.I. Khazin*[†],
 I.A. Koop*, P.P. Krovovny*[†], L.M. Kurdadze*, A.S. Kuzmin*[†],
 I.B. Logashenko*, P.A. Lukin*, A.P. Lysenko*, K.Yu. Mikhailov*,
 A.I. Milstein*[†], I.N. Nesterenko*, V.S. Okhapkin*, A.V. Otboev*,
 E.A. Perevedentsev*[†], A.S. Popov*[†], N.I. Root*[†], A.A. Ruban*,
 N.M. Ryskulov*, A.G. Shamov*, Yu.M. Shatunov*, B.A. Shwartz*[†],
 A.L. Sibidanov*[†], V.A. Sidorov*, A.N. Skrinsky*, V.P. Smakhtin*,
 I.G. Snopkov*, E.P. Solodov*[†], P.Yu. Stepanov*, A.I. Sukhanov*,
 J.A. Thompson[‡], A.A. Valishev*, Yu.V. Yudin*, S.G. Zverev*

Abstract

The cross section of the process $e^+e^- \rightarrow \eta\gamma$ has been measured in the 600-1380 MeV c.m. energy range with the CMD-2 detector. The following branching ratios have been determined:

$$B(\rho \rightarrow \eta\gamma) = (3.28 \pm 0.37 \pm 0.23) \cdot 10^{-4},$$

$$B(\omega \rightarrow \eta\gamma) = (5.10 \pm 0.72 \pm 0.34) \cdot 10^{-4},$$

$$B(\phi \rightarrow \eta\gamma) = (1.287 \pm 0.013 \pm 0.063) \cdot 10^{-2}.$$

Evidence for the $\rho(1450) \rightarrow \eta\gamma$ decay has been obtained for the first time.

*Budker Institute of Nuclear Physics, Novosibirsk, 630090, Russia

[†]Novosibirsk State University, Novosibirsk, 630090, Russia

[‡]University of Pittsburgh, Pittsburgh, PA 15260, USA

[§]Yale University, New Haven, CT 06511, USA

1 Introduction

Radiative decays of the ρ, ω and ϕ and particularly their magnetic dipole transitions to the $\eta\gamma$ final state have traditionally been a good laboratory for various tests of theoretical concepts, from the quark model and SU(3) symmetry to Vector Dominance Model (VDM) and anomalous contributions [1–5]. Among these decays only that of the ϕ meson has been well studied experimentally [6]. However, most of the previous measurements of the $\phi \rightarrow \eta\gamma$ decay were performed in a narrow energy range resulting in a large model uncertainty related to the description of the cross section outside the ϕ meson. This error can be decreased by measuring the cross section in a broader energy range. Experimental information on the ρ and ω decays is rather scarce [6].

The data samples of the $\eta\gamma$ production accumulated previously in the off-resonance region are negligible [7] making impossible the determination of the cross section of the process $e^+e^- \rightarrow \eta\gamma$ which although small could contribute to the total hadronic cross section and thus influence the precision of the calculation of the hadronic contribution to $(g-2)_\mu$ [8].

Large integrated luminosity collected in recent experiments at the VEPP-2M e^+e^- collider in Novosibirsk allows qualitatively new analysis of the $\eta\gamma$ final state produced in e^+e^- annihilation. CMD-2 has already published results of the $\phi \rightarrow \eta\gamma$ study in the $\eta \rightarrow \pi^+\pi^-\pi^0$ decay mode [9] whereas SND presented their determination of the branching ratio of the $\phi \rightarrow \eta\gamma$ decay via various decays modes of the η [10–13] as well as measured the branching ratios of the $\rho, \omega \rightarrow \eta\gamma$ decay in the $\eta \rightarrow 3\pi^0$ decay mode [13]. In this work we report on the measurement of the cross section of the process $e^+e^- \rightarrow \eta\gamma$ in the $\eta \rightarrow 3\pi^0$ decay mode in the broad c.m.energy range 600–1380 MeV as well as determination of the branching ratios of the $\rho, \omega, \phi \rightarrow \eta\gamma$ decay using the CMD-2 detector.

2 Experiment

The general purpose detector CMD-2 has been described in detail elsewhere [14]. Its tracking system consists of a cylindrical drift chamber (DC) and double-layer multiwire proportional Z-chamber, both also used for the trigger, and both inside a thin ($0.38 X_0$) superconducting solenoid with a field of 1 T.

The barrel CsI calorimeter with a thickness of $8.1 X_0$ placed outside the solenoid has the energy resolution for photons of about 9% in the energy range from 100 to 700 MeV. The angular resolution is of the order of 0.02

radians. The end-cap BGO calorimeter with a thickness of $13.4 X_0$ placed inside the solenoid has the energy and angular resolution varying from 9% to 4% and from 0.03 to 0.02 radians respectively for the photon energy in the range 100 to 700 MeV. The barrel and end-cap calorimeter systems cover a solid angle of $0.92 \times 4\pi$ radians.

The experiment was performed in the c.m. energy range 600-1380 MeV during the runs of 1997-2000. The analysis is based on the entire data sample corresponding to 26.3 pb^{-1} .

The step of the c.m. energy scan varied from 500 keV near the ω and ϕ mesons peaks to 5 MeV far from the resonances. The beam energy spread was about 400 keV at 1000 MeV. Luminosity was measured using large angle Bhabha scattering events.

3 Data analysis

To study the process $e^+e^- \rightarrow \eta\gamma$, the decay mode $\eta \rightarrow 3\pi^0$ was chosen so that there are seven photons in the final state.

Some of the photons can escape detection because of the threshold of shower detection, limited solid angle or shower merging. An event can also have additional (“fake”) photons because of the shower splitting, “noisy” crystals in the calorimeter and beam background.

At the first stage of analysis events were selected which had no tracks in the DC, from 6 to 8 photons, the total energy deposition $E_{tot} > 1.5 E_{beam}$, the total momentum $P_{tot} < 0.4 E_{beam}$ and at least 3 photons detected in the CsI calorimeter. The minimum photon energy was 20 MeV for the CsI and 30 MeV for the BGO calorimeter.

After kinematic reconstruction requiring energy-momentum conservation events with good reconstruction quality ($\chi^2 < 12$) and in which for each photon the ratio of the reconstructed energy to the measured one was $0.7 < \omega_i/E_i < 1.9$ were retained.

The detection efficiency for the process under study was determined by Monte Carlo simulation taking into account the neutral trigger efficiency [15]. It rises steeply from 18% at 600 MeV to about 33% at the ϕ meson energy.

Since background conditions strongly vary in the energy range studied, it was divided into three parts:

- low energies — $2E_{beam} < 950 \text{ MeV}$,
- the ϕ meson range — $950 \text{ MeV} < 2E_{beam} < 1060 \text{ MeV}$,
- high energies — $2E_{beam} > 1060 \text{ MeV}$.

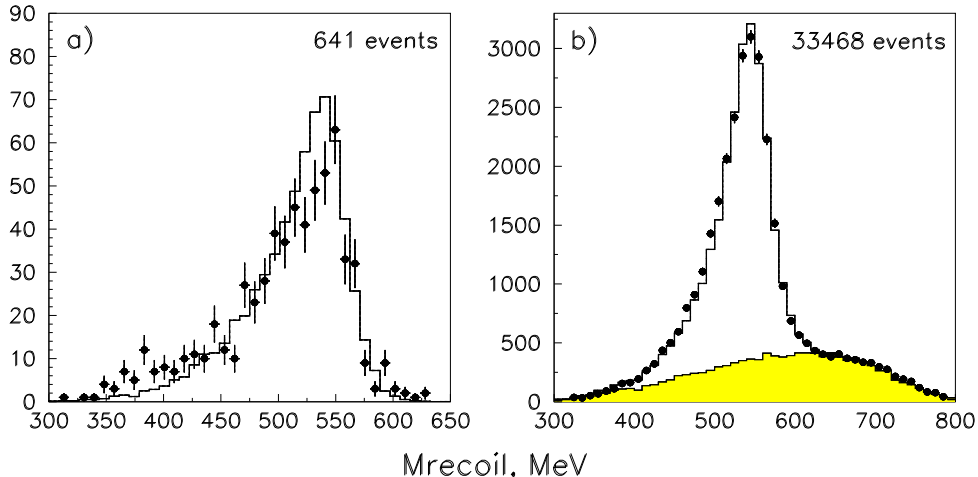


Figure 1: M_{recoil} for the most energetic photon: a) below 950 MeV, b) ϕ meson. Dots correspond to experiment, solid histograms are simulation of the $\eta\gamma$ production, the dashed histogram is background simulation.

Below the $\omega\pi^0$ production threshold ($2E_{beam} < 920$ MeV) there are no other sources of multiphoton events with a significant cross section. Possible background from cosmic muons and QED processes is efficiently suppressed by the cut on the minimum number of photons and total energy deposition. All events meeting the selection criteria were considered as those of the process $e^+e^- \rightarrow \eta\gamma, \eta \rightarrow 3\pi^0$.

In the ϕ meson energy range the main background comes from the decay mode $\phi \rightarrow K_L^0 K_S^0 \rightarrow neutrals$. Since the cross section of this process is large, signal and background events are separated statistically. Outside the ϕ meson there is also a contribution from the process $e^+e^- \rightarrow \omega\pi^0, \omega \rightarrow \pi^0\gamma$.

Separation used the reconstructed recoil mass of the most energetic photon (with the energy ω_1) determined from

$$M_{recoil} = \sqrt{(2E_{beam} - \omega_1)^2 - \omega_1^2}. \quad (1)$$

In Fig. 1 the distribution of the recoil mass for the most energetic photon at low energies and in the ϕ meson range is compared to the simulation. As expected, for $\eta\gamma$ events it exhibits a narrow peak at the η meson mass of 547.3 MeV whereas for background events a broad distribution is observed.

The shape of the background distribution was determined from events with bad reconstruction quality ($\chi^2 > 15$). To this end the M_{recoil} distribution was fit separately for events with six, seven and eight photons using the

function

$$F(z) = A_0 \cdot z^\alpha \cdot (1 - z)^\beta, \quad (2)$$

where $z = (x - x_{min}) / (x_{max} - x_{min})$ and x_{min} and x_{max} are the spectrum boundaries.

For events satisfying the selection criteria, the same distribution was fit by a sum of an asymmetric Gaussian and the background function with the shape fixed as above. After that the shape of the functions was fixed and the fit was performed for all energies.

At high energies where the background is much higher, only events with seven photons were used. A new kinematic fit requiring energy-momentum conservation was performed with the following additional conditions. Five photons with a smaller energy (soft photons) were selected and a kinematic fit to the $\pi^0\pi^0\gamma$ state was required. Thus, three free photons remained: the most energetic or the recoil one, a photon with the second energy and the one which was free among the five soft. The invariant mass of the two latter photons $M_{\gamma\gamma}$ was used for further selection.

After that, good reconstruction quality events ($\chi^2 < 7$) were selected in which for each photon $0.8 < \omega_i / E_i < 1.5$ and $50 < M_{\gamma\gamma} < 200$ MeV. With these cuts the detection efficiency above 1060 MeV is about 8.4%.

Three events have been selected at $2E_{beam} > 1300$ MeV. Figure 2 shows the scatter plot of the recoil mass of the most energetic photon versus the invariant mass $M_{\gamma\gamma}$ of two free photons for these events and simulation of the process $e^+e^- \rightarrow \eta\gamma$.

The main sources of background are the processes:

$$e^+e^- \rightarrow \omega\pi^0, \omega \rightarrow \pi^0\gamma, \quad (3)$$

and

$$e^+e^- \rightarrow \omega\pi^0\pi^0, \omega \rightarrow \pi^0\gamma. \quad (4)$$

The cross section of the process (3) is rather large (about 1.0-1.5 nb), however this process has five final photons only and is easily suppressed by the cut on the minimum number of photons.

The process (4) has seven final photons, six of which pair to three π^0 . Its events can be therefore separated only using the different dynamics of the $\eta\gamma$ and $\omega\pi^0\pi^0$ final states. Its cross section is given by

$$\sigma(e^+e^- \rightarrow \omega\pi^0\pi^0, \omega \rightarrow \pi^0\gamma) = \frac{1}{2}\sigma(e^+e^- \rightarrow \omega\pi^+\pi^-) \cdot B(\omega \rightarrow \pi^0\gamma), \quad (5)$$

so that in the energy range 1300-1400 MeV it is 0.01-0.02 nb according to our measurement of the $\omega\pi^+\pi^-$ production [16].

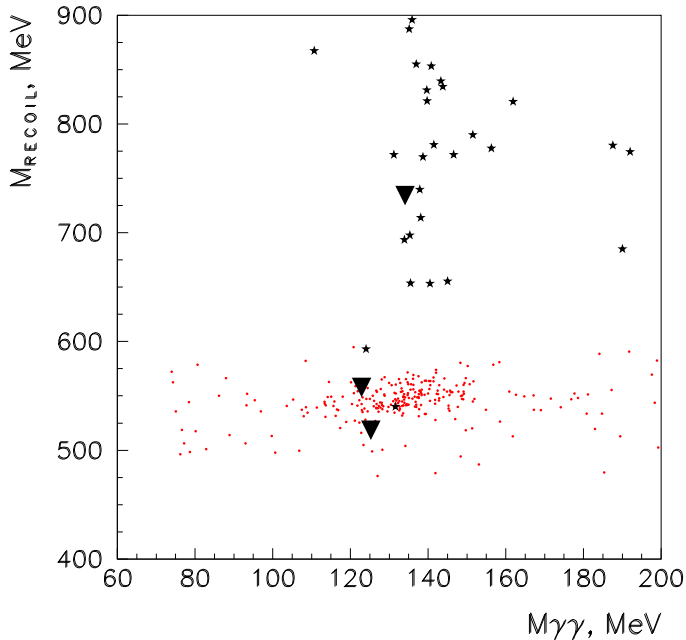


Figure 2: M_{recoil} for the most energetic photon versus $M_{\gamma\gamma}$. Triangles correspond to experiment, dots are the $\eta\gamma$ simulation, stars are the $\omega\pi^0\pi^0$ simulation.

Other possible sources of the background are the radiative return to the ϕ meson with a subsequent decay $\phi \rightarrow \eta\gamma$ and the process $e^+e^- \rightarrow K_L^0 K_S^0 \pi^0$ which have a small cross section and can be also suppressed kinematically.

Simulation shows that in Fig. 2 events of the process $e^+e^- \rightarrow \eta\gamma$ should concentrate in the region $M_{recoil} = M_\eta, M_{\gamma\gamma} = M_{\pi^0}$ whereas those of the background have the broad distribution. Of three observed events two are in the signal region and one is in the background region. The expected number of background events in the whole plot calculated from the cross section above and detection efficiency from Monte Carlo is equal to 1.3 consistent with the observation. This allows the estimation of the contribution from the known background processes to the $\eta\gamma$ region at less than 0.1 event, so that the probability that two observed events in the signal region come from background is less than 0.5%.

4 Results

4.1 Approximation of the cross sections

The energy dependence of the expected number of events is given by:

$$N_{\eta\gamma}^{th} = L(\sqrt{s}) \cdot \tilde{\sigma}(\sqrt{s}) \cdot \epsilon(\sqrt{s}) \cdot B(\eta \rightarrow 3\pi^0) \cdot B^3(\pi^0 \rightarrow 2\gamma), \quad (6)$$

where L is the integrated luminosity at the c.m.energy $\sqrt{s} = 2E_{beam}$, $\tilde{\sigma}$ is the visible cross section of the process $e^+e^- \rightarrow \eta\gamma$, ϵ is the detection efficiency, $B(\eta \rightarrow 3\pi^0) = (32.24 \pm 0.29)\%$ and $B(\pi^0 \rightarrow 2\gamma) = (98.798 \pm 0.032)\%$ are the branching ratios of the corresponding decays [6]. The maximum likelihood method was applied to fit the experimental data to the relation (6) with the parameterization of the cross section described below. The fit took into account the beam energy spread and the uncertainty of the beam energy determination. The radiative corrections were calculated during the fit according to [17]: $\tilde{\sigma}(s)$ is the convolution of the Born cross section $\sigma(s)$ with a probability to emit photons, often simply written as $\tilde{\sigma}(s) = \sigma(s)(1+\delta)$ where δ is referred to as a radiative correction. The dependence of the detection efficiency on the energy of the emitted photon was determined from simulation.

The Born cross section of the process can be written as:

$$\sigma_{\eta\gamma}(s) = \frac{F_{\eta\gamma}(s)}{s^{3/2}} \cdot \left| \sqrt{4\pi\alpha^2} C_\eta + \sum_{V=\rho,\omega,\phi,\rho'} A_V \right|^2, \quad (7)$$

$$A_V = \sqrt{\sigma_V^{(0)} \frac{m_V^3}{F(m_V^2)}} \cdot \frac{m_V \Gamma_V e^{i\varphi_V}}{m_V^2 - s - i\sqrt{s}\Gamma_V(s)},$$

where m_V is the mass of the resonance, $\Gamma_V(s)$ and $\Gamma_V = \Gamma_V(m_V^2)$ are its width at the squared c.m.energy s and at the resonance peak respectively, δ_V is its relative phase, $F(s)$ is a factor taking into account the energy dependence of the phase space of the final state, $F_{\eta\gamma}(s) = p_\eta^3 = (\sqrt{s}(1 - m_\eta^2/2s))^3$, C_η is a possible anomalous contribution, $\sigma_V^{(0)}$ is the cross section at the resonance peak calculated without taking into account other contributions:

$$\sigma_V^{(0)} = \sigma_{e^+e^- \rightarrow V \rightarrow \eta\gamma}(m_V^2) = \frac{12\pi B_{V \rightarrow e^+e^-} B_{V \rightarrow \eta\gamma}}{m_V^2}, \quad (8)$$

where $B_{V \rightarrow e^+e^-}$ and $B_{V \rightarrow \eta\gamma}$ are the corresponding branching ratios.

The Gounaris-Sakurai model has been used for the description of the ρ meson [18]. To describe the energy dependence of the ω and ϕ meson width their main decay modes $\pi^+\pi^-\pi^0$, $\pi^0\gamma$ as well as $K_L^0 K_S^0$, K^+K^- , $\pi^+\pi^-\pi^0$ and $\eta\gamma$ respectively were taken into account as in [19]. For the ρ' the energy

Table 1: Energy, integrated luminosity, detection efficiency, number of selected events, radiative correction and Born cross section of the process $e^+e^- \rightarrow \eta\gamma$.

\sqrt{s} , MeV	L , nb $^{-1}$	ϵ	N	δ	σ , nb
600	57.3	0.182	0	-0.157	< 0.84
630	118	0.197	0	-0.141	< 0.37
660	241	0.211	0	-0.133	< 0.17
690	201	0.224	1	-0.129	$0.08^{+0.10}_{-0.06}$
720	430	0.237	9	-0.125	0.32 ± 0.11
750	216	0.249	7	-0.116	0.47 ± 0.18
760	211	0.253	5	-0.114	0.34 ± 0.15
764	40.7	0.255	1	-0.115	$0.35^{+0.46}_{-0.25}$
770	112	0.257	2	-0.126	$0.26^{+0.23}_{-0.14}$
774	200	0.259	14	-0.149	1.02 ± 0.27
778	204	0.260	22	-0.189	1.64 ± 0.35
780	199	0.261	23	-0.204	1.79 ± 0.37
781	262	0.261	31	-0.204	1.84 ± 0.33
782	646	0.262	103	-0.197	2.45 ± 0.24
783	282	0.262	48	-0.181	2.56 ± 0.37
784	345	0.262	54	-0.158	2.28 ± 0.31
785	204	0.263	24	-0.133	1.66 ± 0.34
786	195	0.263	33	-0.107	2.31 ± 0.40
790	153	0.264	10	-0.032	0.82 ± 0.26
794	183	0.266	14	0.000	0.92 ± 0.25
800	268	0.268	13	0.014	0.57 ± 0.16
810	253	0.272	10	0.017	0.46 ± 0.15
820	303	0.275	8	0.017	0.30 ± 0.11
840	618	0.282	26	0.014	0.47 ± 0.09
880	385	0.294	13	-0.001	0.37 ± 0.10
920	470	0.305	10	-0.035	0.23 ± 0.07
940	336	0.310	8	-0.052	0.26 ± 0.09

Table 2: Energy, integrated luminosity, detection efficiency, number of selected events, radiative correction and Born cross section of the process $e^+e^- \rightarrow \eta\gamma$.

\sqrt{s} , MeV	L , nb $^{-1}$	ϵ	N	δ	σ , nb
950	232	0.313	3	-0.064	0.14 ± 0.08
958	257	0.315	7	-0.075	0.30 ± 0.11
970	256	0.318	5	-0.095	0.23 ± 0.20
984	403	0.321	18	-0.125	0.50 ± 0.17
1004	469	0.325	65	-0.191	1.70 ± 0.28
1010.3	486	0.326	127	-0.226	3.32 ± 0.35
1015.7	442	0.327	534	-0.269	15.97 ± 0.88
1016.78	1040	0.328	1998	-0.278	25.64 ± 0.80
1017.82	1588	0.328	4278	-0.282	36.71 ± 0.90
1018.68	1540	0.328	5773	-0.275	52.14 ± 0.93
1019.69	1456	0.328	5509	-0.240	50.10 ± 0.96
1020.58	924	0.328	2826	-0.183	36.45 ± 1.02
1021.51	477	0.328	955	-0.106	21.49 ± 0.97
1022.74	405	0.329	516	0.009	12.09 ± 0.72
1027.8	530	0.330	212	0.577	2.45 ± 0.39
1033.7	520	0.331	98	1.424	0.75 ± 0.28
1039.6	582	0.332	66	2.503	0.31 ± 0.22
1049.7	452	0.334	35	5.075	$0.12^{+0.21}_{-0.12}$
1060	569	0.335	24	8.552	$0.04^{+0.17}_{-0.04}$
1100	893	0.084	3	16.18	$0.01^{+0.08}_{-0.01}$
1160	1250	0.084	0	4.530	< 0.07
1224	916	0.084	0	0.136	< 0.08
1290	1672	0.084	0	-0.130	< 0.06
1354	1777	0.084	2	-0.149	$0.05^{+0.04}_{-0.03}$

Table 3: $B_{V \rightarrow e^+e^-} B_{V \rightarrow \eta\gamma}$ in various models.

	VDM	VDM + ρ'
$\rho, 10^{-8}$	$1.51 \pm 0.18 \pm 0.10$	$1.61 \pm 0.20 \pm 0.11$
$\omega, 10^{-8}$	$3.62 \pm 0.52 \pm 0.22$	$3.41 \pm 0.52 \pm 0.21$
$\phi, 10^{-6}$	$3.837 \pm 0.041 \pm 0.158$	$3.850 \pm 0.041 \pm 0.159$
$\rho', 10^{-9}$	$\equiv 0$	$3.7^{+2.9}_{-2.0}$
$m_\phi, \text{ MeV}$	$1019.42 \pm 0.04 \pm 0.05$	$1019.40 \pm 0.04 \pm 0.05$
$\chi^2/\text{n.d.f.}$	40.8 / 47	36.4 / 46

dependence of the width assumed 60% and 40% branching ratios for its decays into $a_1(1260)\pi$ and $\omega\pi$ respectively [20].

The detailed information about the experiment including the cross section of the process $e^+e^- \rightarrow \eta\gamma$ and the radiative correction obtained from the fit is presented in Tables 1, 2. The last five energy points combine the whole data sample at $2E_{beam} > 1080$ MeV analyzed with stricter selection criteria. No events were selected in the energy ranges 600 to 660 MeV and 1160 to 1290 MeV, therefore our results are presented as upper limits at 90% C.L. Events selected in the energy range 1025-1100 MeV are mostly due to the radiative return to the ϕ meson as clear from a very high value of the radiative correction δ , so that the uncertainties of the cross section are very large.

4.2 Results of the fits

In all the following fits the cross sections at the resonance peaks $\sigma_\rho^{(0)}$, $\sigma_\omega^{(0)}$, $\sigma_\phi^{(0)}$ as well as the ϕ meson mass m_ϕ are free parameters. Unless otherwise stated, the ρ meson phase is chosen to be $\varphi_\rho = 0^\circ$ while those for the ω and ϕ mesons are $\varphi_\omega = \varphi_\rho$, $\varphi_\phi = \varphi_\rho + 180^\circ$ in agreement with the quark model. The values of other parameters are taken from [6], those of the $\rho(770)$ meson from our measurement [21].

Two different models were considered: the first one is VDM with the ρ , ω , ϕ mesons and in the second one an additional ρ' meson was included. In both cases $C_\eta=0$.

Results of the fits are shown in Table 3 in terms of the product of the branching ratios $B_{V \rightarrow e^+e^-} B_{V \rightarrow \eta\gamma}$ determined from σ_V^0 according to (8) as well as in Fig. 3 together with the fit curves.

Although the fit quality ($\chi^2/\text{n.d.f.}$) in VDM is good, from Fig. 3 it is clear that at $2E_{beam} > 1300$ MeV the measured cross section is not described by the contributions of ρ , ω and ϕ mesons only. This fact provides evidence

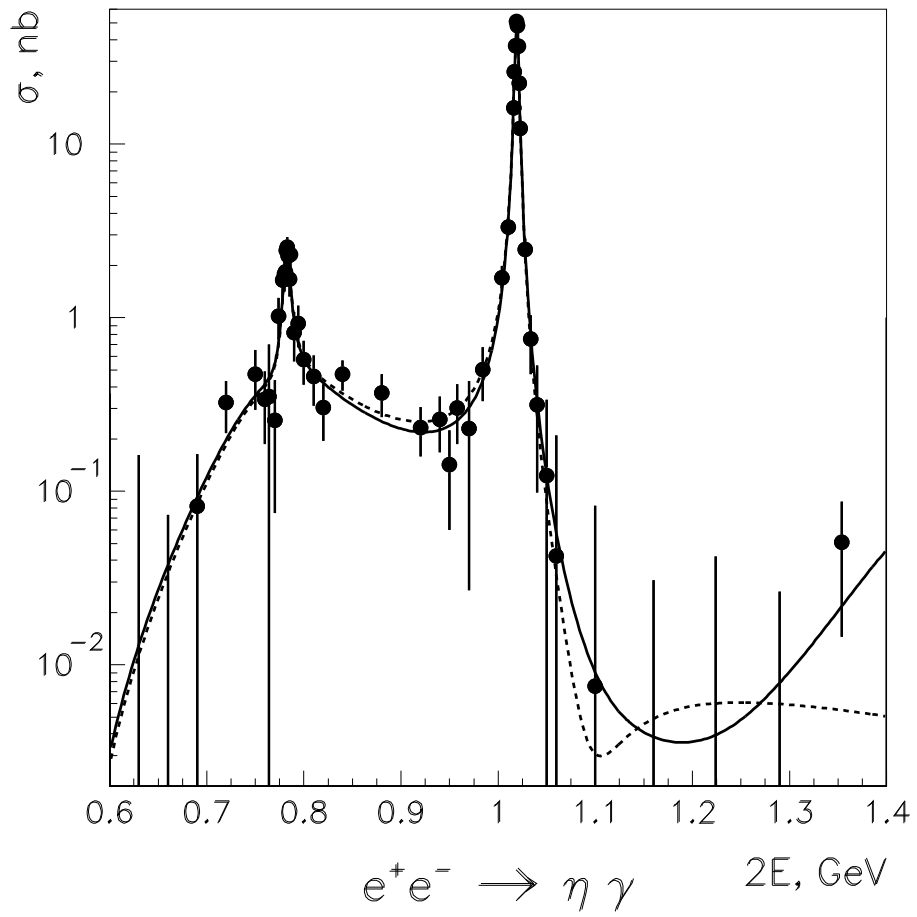


Figure 3: $e^+e^- \rightarrow \eta\gamma$ cross section in the optimal fits: the dashed curve is VDM, the solid one is VDM + $\rho t \rightarrow \eta\gamma$.

for possible additional contributions coming for example from the higher resonances.

In the second model the ρ' mass and width were fixed at 1450 MeV and 310 MeV respectively and the relative phase of the ρ' was fixed at the value of φ_ρ . From Table 3 it can be seen that the agreement with the data is slightly better, mostly due to the high energy point.

One more possibility is to take into account a possible anomalous contribution by adding a nonresonant term determined by the amplitude C_η in the formula (7). C_η is related to the width of the $\eta \rightarrow 2\gamma$ decay [5]. Although this model also provides a good description of the data in the whole energy range including the highest energy point, the high energy behaviour of the anomalous contribution is unknown and the model in its current form is hardly applicable above 1 GeV.

In all models considered the optimal values of the m_ϕ are consistent within errors with the world average value, thus confirming the correctness of the energy scale.

4.3 Systematic errors

The main sources of systematic uncertainties in the cross section determination are listed below:

- Stability to the variation of selection criteria — 5% below 950 MeV, 3.5% from 950 MeV to 1060 MeV, 8% above 1060 MeV;
- The choice of the function describing the recoil photon spectrum at the ϕ meson — 1%;
- The error of the detection efficiency including the neutral trigger efficiency — 1%;
- Determination of the integrated luminosity — 1% in the ϕ meson energy range, 2% at the high energies and 3% below 950 MeV.
- Radiative corrections — 1% for the ω , ϕ and 3% for the ρ meson.

For the determination of the cross section one should additionally take into account the uncertainty of $B_{\eta \rightarrow 3\pi^0}$ equal to 0.9%. Then the systematic uncertainty of the cross sections quoted in Tables 1, 2 is 6.1% below 950 MeV, 4.1% at the ϕ meson and 8.4% above 1060 MeV.

For the determination of the branching fractions $B(V \rightarrow \eta\gamma)$ one should additionally take into account the uncertainty of $B_{V \rightarrow e^+e^-}$ which is 1.8% for the ρ [21] while it is 2.7% for the ω and ϕ [6]. As a result, the systematic uncertainty is 6.9%, 6.6% and 4.9% for ρ , ω and ϕ .

5 Discussion

Although the product of the branching ratios for the ρ' is small and differs from zero by 1.5 standard deviations only, the observed events at high energy can hardly be explained by the known background processes. Moreover, one can independently estimate the cross section of the process $e^+e^- \rightarrow \eta\gamma$ from the measured cross section of the process $e^+e^- \rightarrow \eta\pi^+\pi^-$ [16]. The latter process is known to proceed via the $\eta\rho$ state and one can estimate the $\rho \rightarrow \gamma$ transition from VDM so that

$$\sigma_{\eta\gamma}(E) = \sigma_{\eta\rho}(E) \cdot \frac{4\pi\alpha}{f_\rho^2} \cdot \frac{F_{\eta\gamma}(E)}{F_{\eta\rho}(E)}, \quad (9)$$

where f_ρ is a coupling constant of the ρ meson with a photon which can be obtained from the decay width $\Gamma_{\rho ee} = 4\pi m_\rho \alpha^2 / 3f_\rho^2$; $F_{\eta X}(E)$ is a phase space factor for the ηX final state. The value $\sigma_{\eta\gamma}(1350 \text{ MeV}) = 0.022 \pm 0.004 \text{ nb}$ obtained from (9) at $\varphi_{\rho'} = \varphi_\rho$ is not incompatible with the measured cross section $\sigma_{\eta\gamma}(1350 \text{ MeV}) = 0.051_{-0.028}^{+0.044} \text{ nb}$.

Therefore we consider our observation as evidence for the existence of the $\rho' \rightarrow \eta\gamma$ decay. Since our measurement covers the energy range below 1380 MeV, i.e. the left slope of the ρ' meson only, we can not determine its parameters. However, one can obtain the $e^+e^- \rightarrow \eta\gamma$ cross section in the much broader energy range 1300 to 2450 MeV from the measurements of the cross section $e^+e^- \rightarrow \eta\pi^+\pi^-$ by DM2 [22] and CMD-2 [16] using (9). If the cross sections obtained in such a way are combined with the cross section $e^+e^- \rightarrow \eta\gamma$ from our measurement and a fit is performed with a free mass and width of the ρ' meson, then reasonable description of the whole data is achieved with the following values of resonance parameters:

$$\begin{aligned} B_{\rho \rightarrow e^+e^-} \cdot B_{\rho \rightarrow \eta\gamma} &= (1.52 \pm 0.17 \pm 0.10) \cdot 10^{-8}, \\ B_{\omega \rightarrow e^+e^-} \cdot B_{\omega \rightarrow \eta\gamma} &= (3.60 \pm 0.51 \pm 0.22) \cdot 10^{-8}, \\ B_{\phi \rightarrow e^+e^-} \cdot B_{\phi \rightarrow \eta\gamma} &= (3.849 \pm 0.040 \pm 0.159) \cdot 10^{-6}, \\ B_{\rho' \rightarrow e^+e^-} \cdot B_{\rho' \rightarrow \eta\gamma} &= (10.0 \pm 2.2) \cdot 10^{-9}, \\ m_\phi &= 1019.40 \pm 0.04 \pm 0.05 \text{ MeV}, \\ m_{\rho'} &= 1497 \pm 14 \text{ MeV}, \\ \Gamma_{\rho'} &= 226 \pm 44 \text{ MeV}, \\ \chi^2/\text{n.d.f.} &= 68.9/71. \end{aligned} \quad (10)$$

The cross section $e^+e^- \rightarrow \eta\gamma$ and the obtained fit curve are also shown in Fig. 4 for the energies above 1200 MeV.

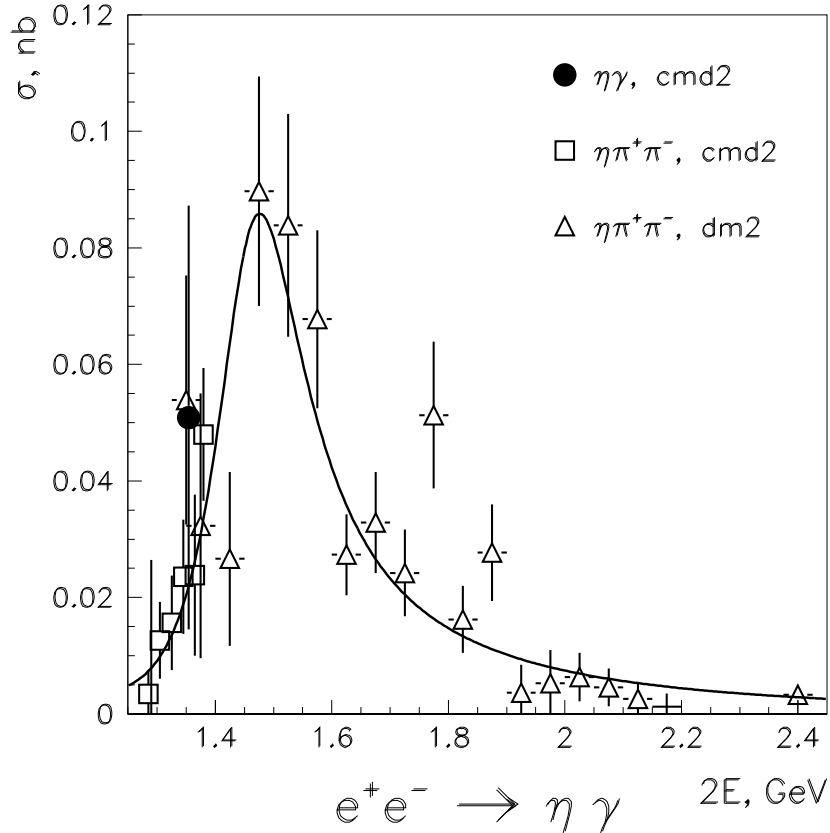


Figure 4: Cross sections: dots are $e^+e^- \rightarrow \eta\gamma$, squares and triangles are results of the calculation from the $e^+e^- \rightarrow \eta\pi^+\pi^-$ production for CMD-2 and DM2 respectively.

Analysis of the fit results in Table 3 as well as those in (10) shows that the model dependence of the branching ratios does not exceed 5% for the ρ and ω mesons whereas for the $\phi \rightarrow \eta\gamma$ decay it is less than 1%. The fit with the ρ' meson gives better description of the data in the whole energy range studied. In all fits described the value of $\chi^2/\text{n.d.f.}$ calculated using our measurement only is practically the same.

The ρ' existence has been well established before in various decay modes [6] and as follows from the analysis above, it can also decay into $\eta\gamma$. Therefore we present the final results in the model with the ρ' meson using both our measurement and the calculation from the cross section of the process $e^+e^- \rightarrow \eta\pi^+\pi^-$.

Table 4: Branching ratios for $\rho, \omega \rightarrow \eta\gamma$ decays.

Experiment	$B(\rho \rightarrow \eta\gamma), 10^{-4}$	$B(\omega \rightarrow \eta\gamma), 10^{-4}$
PDG, 2000 [6]	$2.4^{+0.9}_{-0.8}$	6.5 ± 1.0
SND, 2000 [13]	$2.73 \pm 0.31 \pm 0.15$	$4.62 \pm 0.71 \pm 0.18$
This work, 2001	$3.28 \pm 0.37 \pm 0.23$	$5.10 \pm 0.72 \pm 0.34$

Table 5: Branching ratio of $\phi \rightarrow \eta\gamma$ decay.

Experiment	η decay channel	$B(\phi \rightarrow \eta\gamma), \%$
PDG, 1998 [23]	Average	1.26 ± 0.06
SND, 1998 [10]	$\eta \rightarrow 3\pi^0$	$1.246 \pm 0.025 \pm 0.057$
CMD-2, 1999 [9]	$\eta \rightarrow \pi^+\pi^-\pi^0$	$1.18 \pm 0.03 \pm 0.06$
SND, 1999 [11]	$\eta \rightarrow 2\gamma$	$1.338 \pm 0.012 \pm 0.052$
SND, 2000 [12]	$\eta \rightarrow \pi^+\pi^-\pi^0$	$1.259 \pm 0.030 \pm 0.059$
SND, 2000 [13]	$\eta \rightarrow 3\pi^0$	$1.353 \pm 0.011 \pm 0.052$
This work, 2001	$\eta \rightarrow 3\pi^0$	$1.287 \pm 0.013 \pm 0.063$

The values of the cross section obtained allow the conclusion that above the ϕ meson the contribution of the $\eta\gamma$ production to the total hadronic cross section is negligibly small.

One can use the leptonic branching ratios measured independently to determine the absolute branching ratio $B_{V \rightarrow \eta\gamma}$.

Table 4 compares the branching ratios of the $\rho, \omega \rightarrow \eta\gamma$ decays obtained in this work with the results of SND [13] as well as with the world average values [6].

Table 5 compares the branching ratio of the $\phi \rightarrow \eta\gamma$ decay obtained in this work with the results of the measurements performed before 1998 and listed in the 1998 edition of the Review of Particle Physics [23] as well as with the recent results obtained by two groups at VEPP-2M.

The results of high precision studies of the $\phi \rightarrow \eta\gamma$ decay can be also used to improve the precision of our knowledge of the relative branching ratios of the η meson. It is known that data on the main decay modes of the η meson from different experiments ($\eta \rightarrow 2\gamma, \eta \rightarrow 3\pi^0, \eta \rightarrow \pi^+\pi^-\pi^0$) [6] are not consistent with each other and their averaging requires a scale factor of 1.2-1.3. CMD-2 performed two independent measurements of the $B(\phi \rightarrow \eta\gamma)$ using η decays into $\pi^+\pi^-\pi^0$ [9] and $3\pi^0$ allowing the determination of the ratio $B(\eta \rightarrow 3\pi^0)/B(\eta \rightarrow \pi^+\pi^-\pi^0)$. In such a ratio some of the systematic uncertainties cancel (e.g. the error of $B_{\phi \rightarrow e^+e^-}$, uncertainty of luminosity

determination).

Using the value of $B(\phi \rightarrow \eta\gamma) = (1.18 \pm 0.03 \pm 0.06) \%$, obtained in [9], one can determine

$$\frac{B(\eta \rightarrow 3\pi^0)}{B(\eta \rightarrow \pi^+\pi^-\pi^0)} = 1.52 \pm 0.04 \pm 0.08, \quad (11)$$

which is compatible with all previous measurements [6] and has better accuracy. The accuracy of our result is also better than that of the world average:

$$\frac{B(\eta \rightarrow 3\pi^0)}{B(\eta \rightarrow \pi^+\pi^-\pi^0)} = 1.34 \pm 0.10. \quad (12)$$

6 Conclusions

The following results were obtained by the CMD-2 detector:

- Using a data sample corresponding to the integrated luminosity of 26.3 pb^{-1} the cross section of the process $e^+e^- \rightarrow \eta\gamma$ was measured in the c.m.energy range 600-1380 MeV.
- The Vector Dominance Model extended by introducing a ρ' meson decaying to $\eta\gamma$ can well describe the data. The cross sections in the peak as well as the branching ratios of ρ, ω and ϕ decay into $\eta\gamma$ were determined. Evidence for the $\rho' \rightarrow \eta\gamma$ decay was obtained for the first time.
- Measurement of the $B(\phi \rightarrow \eta\gamma)$ by one detector in two decay modes of the η allows the determination of the ratio:

$$\frac{B(\eta \rightarrow 3\pi^0)}{B(\eta \rightarrow \pi^+\pi^-\pi^0)} = 1.52 \pm 0.04 \pm 0.08,$$

compatible with the world average and surpassing it in accuracy.

The authors are grateful to the staff of VEPP-2M for the excellent performance of the collider, to all engineers and technicians who participated in the design, commissioning and operation of CMD-2. We acknowledge useful and stimulating discussions with N.N.Achasov, M.Benayoun, A.V.Berdyugin and V.L.Chernyak.

References

- [1] P. O'Donnell, *Rev. Mod. Phys.* **53** (1981) 673.
- [2] G. Morpurgo, *Phys. Rev.* **D42** (1990) 1497.
- [3] M. Hashimoto, *Phys. Rev.* **D54** (1996) 5611.
- [4] M. Benayoun *et al.*, *Phys. Rev.* **D42** (1999) 114027.
- [5] M. Benayoun, S.I. Eidelman and V.N. Ivanchenko, *Z. Phys.* **C72** (1996) 221.
- [6] D.E. Groom *et al.*, *Eur. Phys. J.* **C15** (2000) 1.
- [7] S.I. Dolinsky *et al.*, *Phys. Reports* **C202** (1991) 99.
- [8] S. Eidelman and F. Jegerlehner, *Z. Phys.* **C67** (1995) 585.
- [9] R.R. Akhmetshin *et al.*, *Phys. Lett.* **B460** (1999) 242.
- [10] M.N. Achasov *et al.*, *JETP Lett.* **68** (1998) 573.
- [11] M.N. Achasov *et al.*, *Eur. Phys. J.* **C12** (2000) 25.
- [12] M.N. Achasov *et al.*, *JETP* **90** (2000) 17.
- [13] M.N. Achasov *et al.*, *JETP Lett.* **72** (2000) 282.
- [14] G.A. Aksenov *et al.*, Preprint Budker INP 85-118, Novosibirsk, 1985.
E.V. Anashkin *et al.*, *ICFA Instr. Bulletin* **5** (1988) 18.
- [15] P.P. Krokovny, Master's Thesis, Novosibirsk State University, 2000.
- [16] R.R. Akhmetshin *et al.*, *Phys. Lett.* **B489** (2000) 125.
- [17] E.A. Kuraev and V.S. Fadin, *Sov. J. Nucl. Phys.*, **41** (1985) 466.
- [18] G.J. Gounaris and J.J. Sakurai, *Phys. Rev. Lett.* **21** (1968) 244.
- [19] R.R. Akhmetshin *et al.*, *Phys. Lett.* **B434** (1998) 426.
- [20] R.R. Akhmetshin *et al.*, *Phys. Lett.* **B466** (1999) 392.
- [21] R.R. Akhmetshin *et al.*, Preprint Budker INP 99-10, Novosibirsk, 1999.
e-Print Archive: hep-ex/9904027.
- [22] A. Antonelli *et al.*, *Phys. Lett.* **B212** (1988) 133.
- [23] C. Caso *et al.*, *Eur. Phys. J.* **C3** (1998) 1.